Corrosion Behavior of V_2AlC and Cr_2AlC MAX phase Materials in 0.01N NaCl

Rana Afif Majed[1], Ahmed M. Al-Ghaban[2], Russul F. Faleh

1 University of technology, Materials Engineering Department
Baghdad, Iraq
Email: Dr.Rana.A.Anaee {at} uotechnology.edu.iq
2 University of technology, Materials Engineering Department
Baghdad, Iraq

ABSTRACT— ***This work involves the manufacturing of MAX phase materials include V_2AlC and Cr_2AlC using powder metallurgy as a new class of materials which characterized by regular crystals in lattice. Corrosion behavior of these materials was investigates by Potentiostat to estimate corrosion resistance in 0.01N of NaCl at four temperatures in the range of 30–60^oC. The results of corrosion resistance indicate that Cr_2AlC has more resistance than V_2AlC in experimental electrolyte due to protective film of α-Al_2O_3 and Cr_2O_3 which are formed on the surface, and both MAX materials are more resistance than SS 316L (which acts as the most corrosion resistance alloy), i.e., the new class of materials which refer to MAX have good corrosion resistance in addition to good thermal, physical, electrical and mechanical properties that reviewed in many literatures. Cyclic polarization test exhibits no chance to pitting corrosion in MAX phase materials in 0.01N NaCl solution. Optical microscopy confirms the good corrosion resistance of Cr_2AlC compared with V_2AlC material.***

Keywords— MAX phase materials, Corrosion behavior, V_2AlC, Cr_2AlC.

---

1. INTRODUCTION

The $M_{N+1}AX_N$ Phases: A New Class of Solids; “Thermodynamically Stable Nanolaminates”. A “nanolaminate” is a material with a laminated – layered – structure in which the thicknesses of the individual layers are in the nanometer range. In principle, a MAX phase does not necessarily have to be thermodynamically stable. The term “thermodynamically stable nanolaminates” was used to distinguish them from *artificial* nanolaminates, e.g., superlattice thin films. An equivalent, but more stringent, description to “thermodynamically stable nanolaminates” is to refer to the MAX phases as “inherently nanolaminated” (i.e., they are nanolaminated by nature, not by artificial design). Note, however, that these terms are not restricted to the MAX phases, but include many other phases with a laminated structure [1,2]. Many authors were interested fabrication of MAX phase materials and studied of some their physical and mechanical properties such as the electronic and structural properties of the layered ternary compound Ti_3AlC_2 using the ab initio pseudopotential method based on density functional theory [3]. Also the isothermal oxidation behavior of Ti_2AlC at intermediate temperatures of 500, 600, 700, 800, and 900°C in flowing air by means of thermogravimetric analysis, X-ray diffraction (XRD), Raman spectroscopy, and scanning electron microscopy (SEM)/energy dispersive spectroscopy[4] and TEM [5] was investigated.

Theoretical studies of the bulk modulus of M_2AlC, where M_5Ti, V, Cr by means of *ab initio* total energy calculations using the projector augmented wave methods were performed. The bulk modulus of M_2AlC increases as Ti is substituted with V and Cr by 19% and 36%, respectively. This can be understood since the substitution of Ti by V and Cr is associated with an extensive increase in the M–Al and M–C bond energy [6]. The equilibrium volume and the density of states (DOS) of Cr_2AlC for antiferromagnetic (AFM), ferromagnetic (FM) and paramagnetic (PM) configurations by ab initio total energy calculations were calculated based on a comparison of the cohesive energies as well as the DOS for all three magnetic configurations. The charge density distribution suggests that the chemical bonding between Cr and C in Cr_2AlC is very similar to the one in cubic CrC [7]. The electronic, magnetotransport, thermoelectric, thermal, and elastic properties of four M_2AlC phases: Ti_2AlC, V_2AlC, Cr_2AlC and Nb_2AlC were investigated [8].

Cr_2AlC ceramics by hot-pressing using Cr, Al and C powders as starting materials were fabricated. The phase assemblages of the samples consisted of Cr_2AlC, as a major crystalline phase, together with a very small amount of Cr_7C_3 and an unknown phase. Its thermal and electrical as well as mechanical properties were determined [9], The hardness, Young’s modulus, flexural strength, and compressive strength of Cr_2AlC samples were 5.2, 288 GPa, 483729, and 1159723 MPa, respectively, which are comparable with those of Ti_3AlC_2 and Nb_2AlC. The material exhibits good damage tolerance [10]. The electronic structure of $Ta_{n+1}AlC_n$ (space group *P63/mmc*, n = 1–3) under uniform compression from 0 to 60 GPa and at temperatures from 0 to 1500 K using *ab initio* calculations was calculated [11]. The crystal structures of new phases compounds, $(V_{0.5}Cr_{0.5})_3AlC_2$, $(V_{0.5}Cr_{0.5})_4AlC_3$, and $(V_{0.5}Cr_{0.5})_5Al_2C_3$ by reactive hot pressing V, Cr, Al, and graphite powders were determined using a combination of X-ray diffraction and scanning transmission electron microscopy [12].

The isothermal oxidation behavior of Cr_2AlC ceramics oxidized in air at 1100 and 1250 ^oC for 20 h [13] and the compressive properties of ternary compound Cr_2AlC at different temperatures and strain rates [14] were studied. The dense bulk Cr_2AlC behave good electrical and thermal conductor [15]. Chemical and oxidation resistances as well as mechanical properties at high temperatures of Cr_2AlC ternary carbide were studied [16]. There are little studies about the corrosion behavior of MAX phase materials.

The aim of present work is fabricate the V_2AlC and Cr_2AlC materials by powder metallurgy and study the thermodynamic functions of their corrosion behavior in sodium chloride with 0.01N concentration and comparison their behavior with Stainless Steel 316L which act as most metallic resistant alloys at four temperatures 30, 40, 50 and 60^{o}C. The electrolyte of 0.01N NaCl was selected due to corrosivity of chloride ions and its effect to accelerate pitting corrosion.

2. EXPERIMENTAL PROCEDURE

To fabricate the V_2AlC and Cr_2AlC samples V, Cr, C, and Al powders (99% pure) were mixed in stoichiometric proportions, ball milled (BAIRD & TATLOCK) for 20 min at high level of speed for each sample, cold pressed using the hydraulic press machine type (Mega 50 Ton Max) and placed in a graphite die in a vacuum hot press (MTI Corporation GLS 1500X). The latter was evacuated and heated to 1100-1350 °C for 6 h. The sample was held at the maximum applied uniaxial pressure ~3 ton for 10 min.

To characterize the prepared MAX phase material, X-ray Diffraction (XRD) analysis was used in order to find out the composition and phase identification of each sample using Shimadzu X-ray diffractometer (type XRD- 6000/7000).

Electrochemical measurements were performed with a potentiostat by SCI electrochemical software at a scan rate 5 $mV.sec^{-1}$. Polarization experiments were started when the rate at which open circuit potential (E_{ocp}) changed was less and more 300mV. The main results obtained were expressed in terms of the corrosion potentials (E_{corr}) and corrosion current density (i_{corr}) in addition to measure the Tafel slops by Tafel extrapolation method. From the values of Tafel slopes and corrosion current density, the polarization resistances values can be calculate according to Stern-Geary equation.

0.01N NaCl solution (pH=7) was used for corrosion tests. All experiments were achieved at four temperatures which adjusted by water bath which randomly selected. The microstructure evolution was investigated by means of optical microscope using (BEL photonics) microscope was connected to computer

3. RESULTS AND DISCUSSION

The X-ray powder diffraction patterns collected at 1 atm for V_2AlC and Cr_2AlC are shown in Figures (1) and (2). For two materials, all major peaks were assigned to the hexagonal structure with the space group *P*63 /*mmc*. A few low intensity impurity peaks were not identified. XRD test good agreement with observed test by Bouchaib [17].

Figures (3) to (5) show the potential – time measurements for V_2AlC, Cr_2AlC and SS 316L for 600 sec respectively at scan rate 5 $mV.sec^{-1}$, these relationships indicate the variation of potentials for Cr_2AlC and SS 316L compared with V_2AlC material which may be attributed to breakdown and repair of protective film on the surfaces of Cr_2AlC and SS 316L materials in 0.01N NaCl solution. The potential of the sample was followed as a function of time in order to study the evolution of the film chemistry as it came to equilibrium with the solution.

Figures (6) to (8) show the Tafel plots of V_2AlC, Cr_2AlC and SS 316L respectively; these curves show the cathodic and anodic behavior of experimental materials. The breakdown and repair of protective film on the Cr_2AlC surface was clearly noticed in the Tafel plot which means that there are protective films may be formed on the Cr_2AlC surface in NaCl solution especially at cathodic region, this result good agreement with the observations which made by Dong et al. who reveal that the Cr_2AlC compounds were resistant to corrosion because a thin α-Al_2O_3 barrier layer quickly formed on the surface which suppressed sulfidation. The superior corrosion resistance of Cr_2AlC originated from the high affinity of Al for oxygen to form the thermodynamically stable Al_2O_3. Unlike Al, Cr was not active because Cr was strongly bound to carbon as Cr_2C layers in Cr_2AlC. The small amount of Cr_2O_3 that had formed was dissolved in the Al_2O_3 layer. The corrosion of Cr_2AlC resulted in the formation of an α-Al_2O_3 layer and an underlying Cr_7C_3 layer [18].

The reduction reaction in neutral solution represents by reduction of oxygen as shown below, on the other hand the oxygen tend to form protective passive film of Al_2O_3 and Cr_2O_3.

$$O_2 + 2H_2O + 4e \rightarrow 4OH^- \qquad \ldots\ldots (1)$$

Corrosion parameters which listed in Table (1) indicate that the corrosion current densities take the following order:

$$\boldsymbol{i_{corr}\ in\ 0.01N\ NaCl \qquad Cr_2AlC < V_2AlC < SS\ 316L}$$

This order was good agreement with the result of polarization resistance value that listed in Table (1).

The polarization resistance (R_p) may be defined as the slope of a potential (ΔE)-current density (Δi). The term (R_p) corresponds to the resistance (R) of the metal/solution interface to charge –transfer reaction. It is also a measure of the resistance of the metal to corrosion in the solution in which the metal is immersed. The polarization resistance (R_p) can be determined from Stern- Geary equation:

$$R_p = \left(\frac{dE}{di}\right)_{i=0} = \frac{b_a * b_c}{2.303 * i_{corr} * (b_a + b_c)} \quad ....(2)$$

where b_c and b_a are cathodic and anodic Tafel slop respectively. The values of R_p are presented in Table (1). These data indicate that the polarization resistance was good agreement with the results of corrosion current density. Also the data of polarization resistance enhanced the corrosion behavior of MAX phase materials which is better than SS 316L due to regular crystals in structures and formation of thermodynamically stable nanolaminates.

The cyclic polarization of tested materials shows no chance to pitting, which is recognized as a dangerous form of corrosion, in tested media as shown in Figures (9) to (11). This means that V_2AlC and Cr_2AlC materials were exhibited a good resistance to corrosion in 0.01N of NaCl solution at different temperatures in the range of 30 – 60^{o}C.

Optical microscopies enhanced the resistivity of MAX phase materials to corrosion in 0.01N NaCl solution. Figure (12) shows the polished and corroded surface of V_2AlC and Cr_2AlC materials at 10X. These images indicate the homogenous surface for both MAX materials. The microstructure test of Cr_2AlC shows the formation of this phase, in addition to form Cr_2C_3 (dark region) and Cr_7C_3 phase can be found (white region) [19]. After corrosion test, we can see the delamination in V_2AlC material compared with Cr_2AlC which exhibit little change in homogeneity of surface.

In Crystallography and defects, corrosion results in the removal of atoms from a metal by dissolution or conversion to an oxidized phase, such as an oxide or sulfide. The metal atoms most likely to undergo corrosion are those with the highest free energy. Thus, atoms located within the bulk of the material are much less susceptible to corrosion than those in the outermost layers of the metal surface, and corrosion reactions are generally considered to be surface chemistry [20].

4. REFERENCES

[1] R.M. Brick, R.B. Gordon, and A. Phillips, *Structure and Properties of Alloys*, McGraw-Hill, 1965.

[2] L.S. Van Delinder, Ed., *Corrosion Basics--An Introduction*, National Association of Corrosion Engineers, 1984.

[3] Y. C. Zhou, X. H. Wang, Z. M. Sun and S. Q. Chen, "Electronic and structural properties of the layered ternary carbide Ti_3AlC_2", *J. Mater. Chem.*, 2001, 11, 2335–2339.

[4] X.H. Wang and Y.C. Zhou, "Intermediate-temperature oxidation behavior of Ti_2AlC in air", *J. Mater. Res.*, Vol. 17, No. 11, Nov 2002

[5] X.H. Wang, Y.C. Zhou, "Microstructure and properties of Ti_3AlC_2 prepared by the solid–liquid reaction synthesis and simultaneous in-situ hot pressing process", *Acta Materialia*, 50 (2002) 3141–3149

[6] Zhimei Sun, Rajeev Ahuja and Sa Li, and Jochen M. Schneider, "Structure and bulk modulus of M2AlC .MÄTi, V, and Cr", *Appl. Phys. Lett.*, Vol. 83, No. 5, 4 August 2003.

[7] Jochen M. Schneidera,, Zhimei Suna, Raphael Mertensa, Fatih Uestela, and Rajeev Ahujac, "Ab initio calculations and experimental determination of the structure of Cr_2AlC", *Solid State Communications* 130 (2004) 445–449.

[8] J. D. Hettinger, S. E. Lofland, P. Finke, T. Meehan, J. Palma, K. Harrell, S. Gupta, A. Ganguly, T. El-Raghy, and M. W. Barsoum, "Electrical transport, thermal transport, and elastic properties of M_2AlC (M=Ti, Cr, Nb, and V)", *Physical Review* B 72, 115-120, 2005.

[9] Wubian Tian, Peiling Wang, Guojun Zhang, Yanmei Kan, Yongxiang Li, and Dongsheng Yan, "Synthesis and thermal and electrical properties of bulk Cr_2AlC", *Scripta Materialia*, 54 (2006) 841–846.

[10] Wu-bian Tian, Pei-ling Wang, Guo-jun Zhang, Yan-mei Kan, and Yong-xiang Li, "Mechanical Properties of Cr_2AlC Ceramics", *J. Am. Ceram. Soc.*, 90 [5] 1663–1666 (2007).

[11] Denis Music, Jens Emmerlich and Jochen M Schneider, "Phase stability and elastic properties of $Ta_{n+1}AlC_n$(n = 1–3) at high pressure and elevated temperature", *J. Phys.: Condens. Matter*, 19 (2007) 136207 (9pp)

[12] Yanchun Zhou, Fanling Meng, and Jie Zhang, "New MAX-Phase Compounds in the V–Cr–Al–C System", *J. Am. Ceram. Soc.*, 91 [4] 1357–1360 (2008).

[13] Wubian Tian, Peiling Wang, Yanmei Kan, and Guojun Zhang, "Oxidation behavior of Cr_2AlC ceramics at 1100 and 1250^{o}C", *J Mater Sci.*, (2008) 43:2785–2791.

[14] Wubian Tian, ZhengMing Sun, and Hitoshi Hashimoto, "Compressive deformation behavior of ternary compound Cr_2AlC", *J Mater Sci*, (2009) 44:102–107.

[15] W.B Zhou, B.C. Mei, and J.Q. Zhu, "On the synthesis and properties of bulk ternary Cr_2AlC ceramics", *Materials Science-Poland*, Vol. 27, No. 4/1, 2009.

[16] Chang-Sam Kim, Sung Ik Hwang, Jung-Soo Ha, Seung-Min Kang and Deock-Soo Cheong, "Synthesis of a Cr_2AlC-Ti_2AlC ternary carbide", *Journal of Ceramic Processing Research.* Vol. 11, No. 1, pp. 82-85 (2010).

[17] Bouchaib Manoun, "Compression behavior of M_2AlC (M=Ti, V, Cr, Nb, and Ta) phases to above 50 GPa", *PHYSICAL REVIEW B*, 73, 024110, 2006.

[18] Dong Bok Lee, Thuan Dinh Nguyen, and Sang Whan Park, "Corrosion of Cr_2AlC in Ar/1%SO_2 Gas Between 900 and 1200 °C", *Oxidation of Metals*, Vol.75, Issue 5-6, pp 313-323, June 2011.

[19] Mohamad Riza Iskandar, " Growth Mechanisms and Microstructure Evolution of MAX phases Thin Films and of Oxide Scales on High Temperature Materials", M.Sc. Thesis, 15. November 2011.
[20] *Cor
rosion: Fundamentals, Testing, and Protection* was published in 2003 as Volume 13A of the *ASM Handbook*. The Volume was prepared under the direction of the ASM Handbook Committee.

Table 1: Corrosion parameters for V_2AlC, Cr_2AlC and SS316L in 0.01N NaCl at four temperatures.

Material	***Temp. °C***	$-E_{oc}$ ***mV***	$-E_{corr}$ ***mV***	i_{corr} $\mu A.cm^{-2}$	$-b_c$ $mV.dec^{-1}$	$+b_a$ $mV.dec^{-1}$	$R_p\ x10^3$ $\Omega.cm^2$
V_2AlC	30 40 50 60	395 570 644 653	448.5 621.8 686.3 690.8	6.97 9.02 10.72 11.54	92.7 104.9 115.1 123.2	91.1 79.6 92.2 84.5	2.862 2.179 2.074 1.886
Cr_2AlC	30 40 50 60	557 548 569 604	528.0 511.0 537.6 665.5	3.80 5.25 9.02 9.89	99.9 102.5 289.7 275.8	209.6 93.9 252.5 234.6	7.731 4.053 6.495 5.566
SS 316L	30 40 50 60	537 513 547 571	544.1 513.9 574.8 611.7	15.17 17.83 18.37 19.82	189.2 156.4 204.9 197.7	140.4 124.1 153.3 181.2	2.307 1.685 2.073 2.071

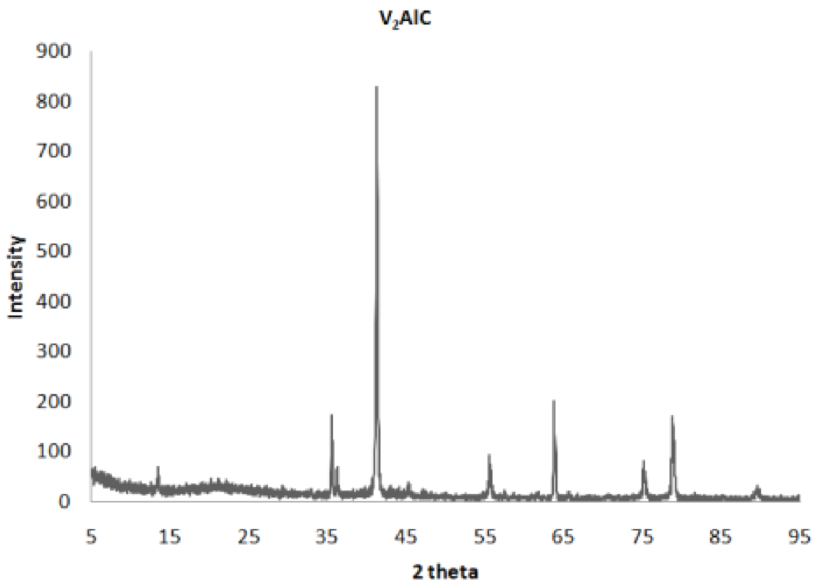

Figure 1: XRD for prepared V_2AlC material.

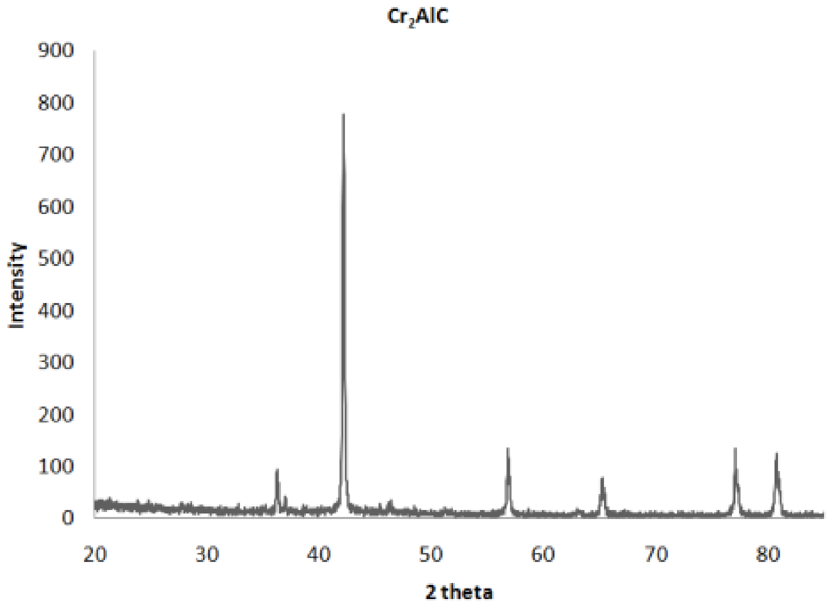

Figure 2: XRD for prepared Cr_2AlC material.

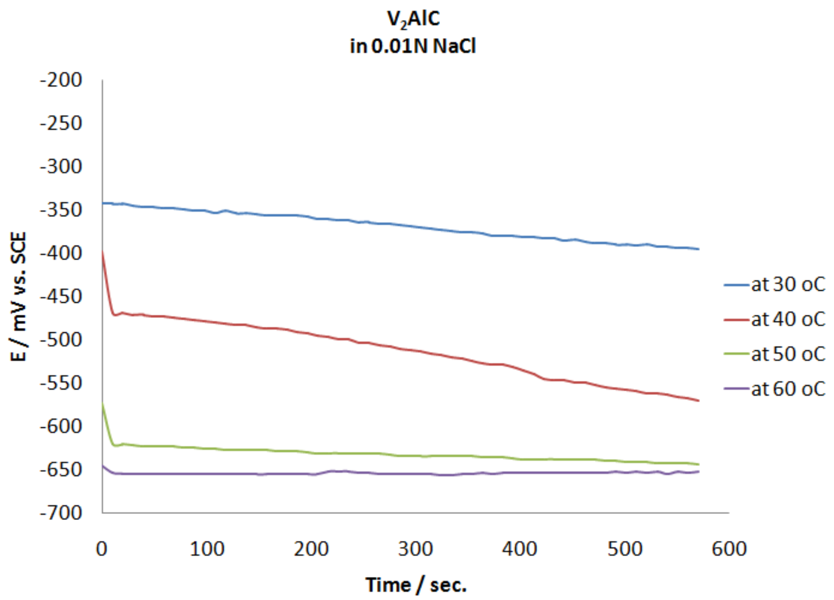

Figure 3: Potential – time measurements of V_2AlC.

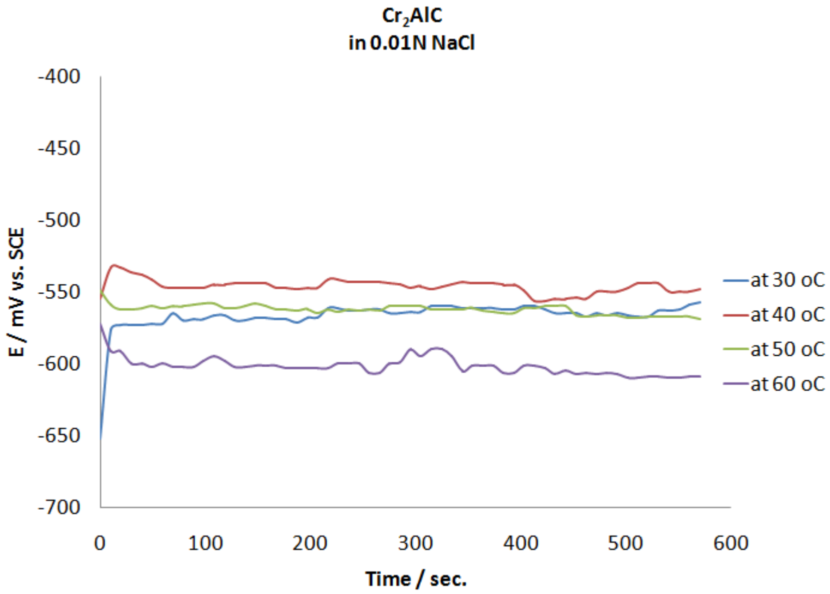

Figure 4: Potential – time measurements of Cr_2AlC.

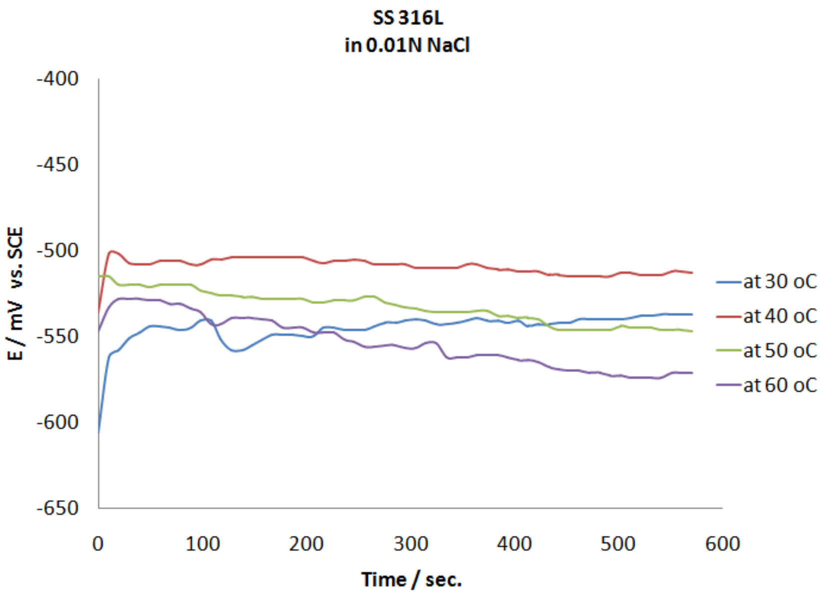

Figure 5: Potential – time measurements of SS 316L.

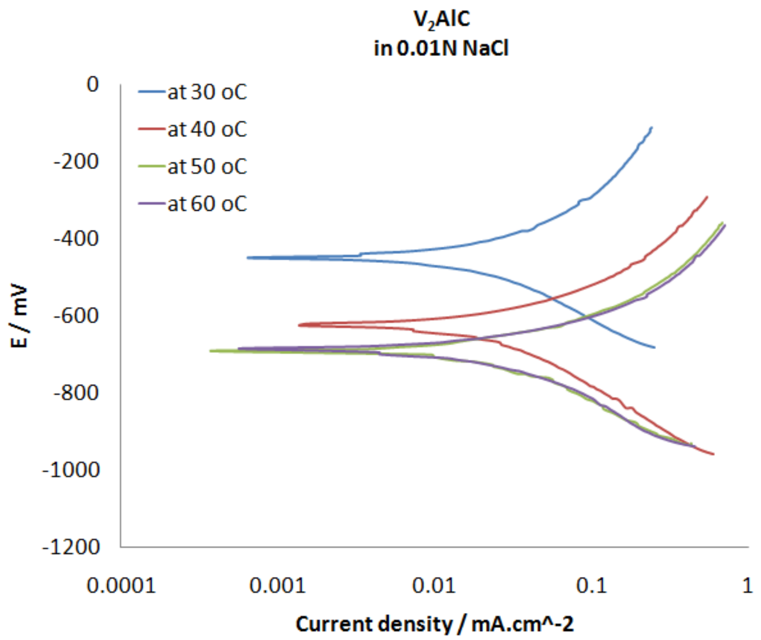

Figure 6: Tafel plot of V_2AlC.

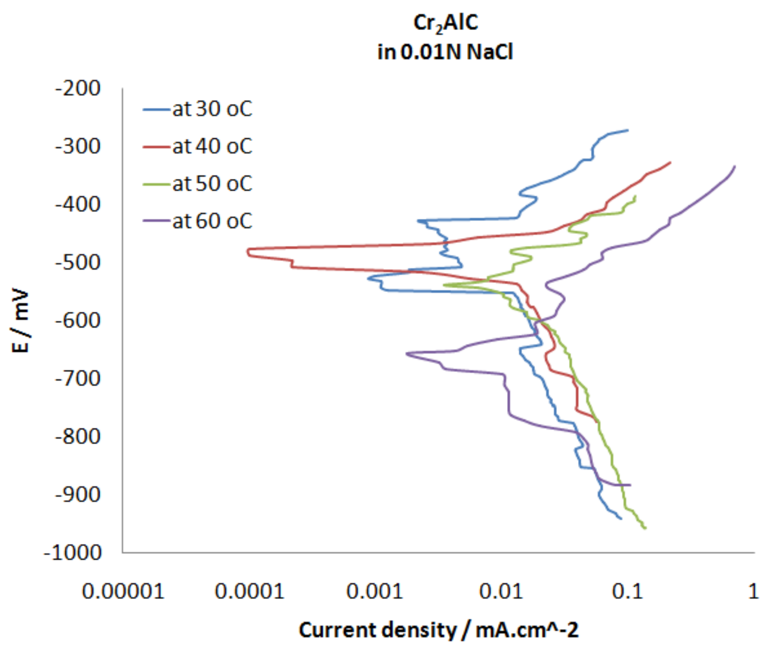

Figure 7: Tafel plot of Cr_2AlC.

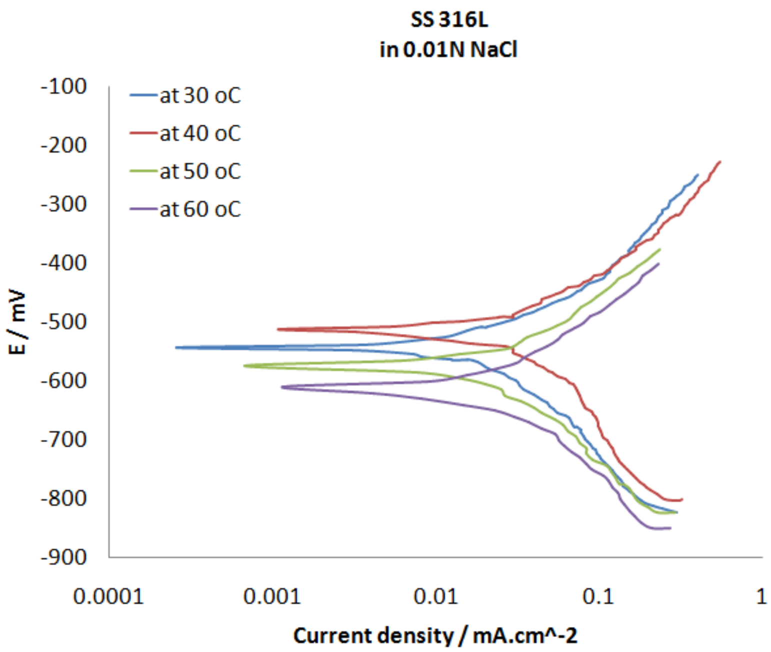

Figure 8: Tafel plot of SS 316L.

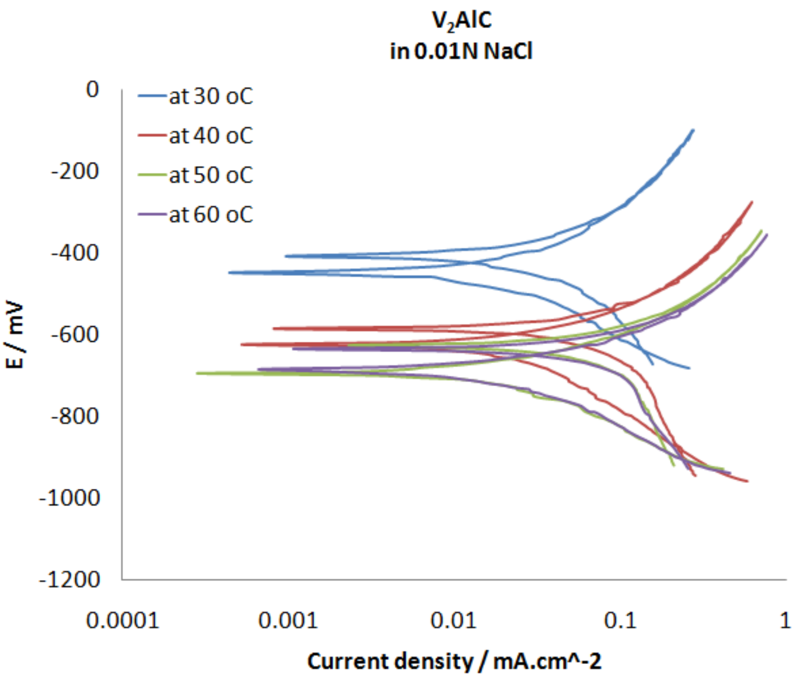

Figure 9: Cyclic polarization of V_2AlC.

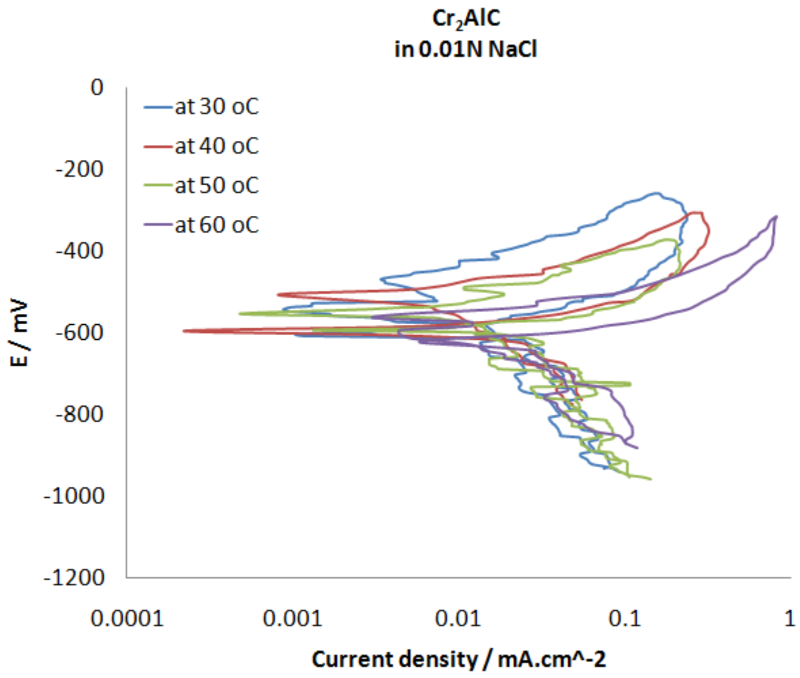

Figure 10: Cyclic polarization of Cr_2AlC.

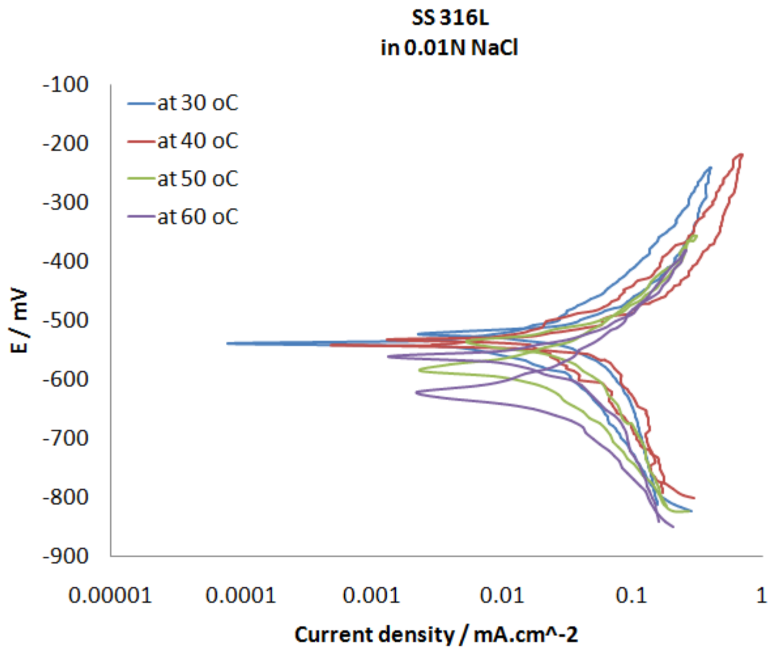

Figure 11: Cyclic polarization of SS 316L.

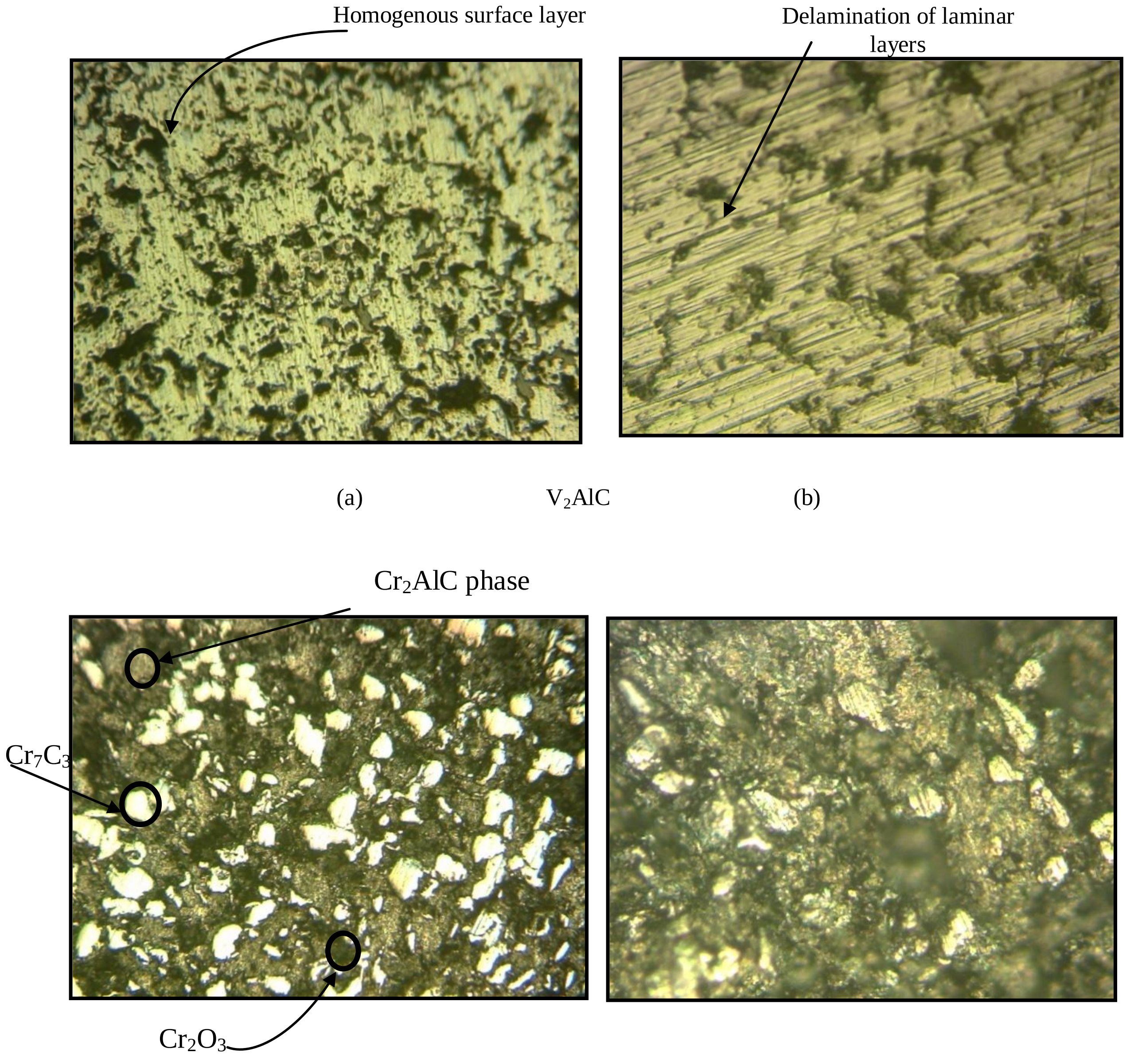

Figure 12: Optical microstructure for polished (a); and corroded (b) surfaces of MAX phases material 0.01N NaCl medium at 10X.